CSIRO PUBLISHING

International Journal of Wildland Fire **2010**, *19*, 202–212 www.publish.csiro.au/journals/ijwf

A sub-grid, mixture–fraction-based thermodynamic equilibrium model for gas phase combustion in FIRETEC: development and results

Michael M. Clark[A,B,C], *Thomas H. Fletcher*[A] *and Rodman R. Linn*[B]

[A]Department of Chemical Engineering, Brigham Young University, Provo, UT 84602, USA.
[B]Earth and Environmental Sciences Division, Los Alamos National Laboratory, Los Alamos, NM 87545, USA.
[C]Corresponding author. Email: mmclark@byu.net

Abstract. The chemical processes of gas phase combustion in wildland fires are complex and occur at length-scales that are not resolved in computational fluid dynamics (CFD) models of landscape-scale wildland fire. A new approach for modelling fire chemistry in HIGRAD/FIRETEC (a landscape-scale CFD wildfire model) applies a mixture–fraction model relying on thermodynamic chemical equilibrium to predict combustion flame temperatures and product species compositions. The mixture–fraction approach is common in combustor modelling applications. However, since individual flame sheets are not resolved in HIGRAD/FIRETEC, application of the mixture–fraction approach requires the development of a sub-grid model, which is based on the two assumptions (i) that combustible gases are concentrated into distinct pockets surrounded by air and combustion products and (ii) that reaction is limited by the mixing of the surrounding air with combustible gases from these pockets. The pocket radius and the thickness of the mixing zone are key parameters used in this model to characterise the sub-grid region where reaction occurs. The development of this sub-grid gas phase model is presented along with simulation results for various types of vegetation, including grass, California chaparral and ponderosa pine.

Introduction

The phenomena of wildfires are fascinating, powerful and extremely complex. With the advent of modern computing, the attempt is made to predict wildfire behaviour using numerical models in order to provide a useful tool for understanding wildfire behaviour. Current operational wildfire models in the United States are based on empirical models (Rothermel 1972; Finney 1998; Andrews *et al*. 2003). These models are point-functional in that they predict fire spread rate at a point using correlations based on local conditions (i.e. wind velocity, fuel moisture content, slope, etc.) Operational models are useful tools for fire managers; however, they do not treat the dynamic coupling of wildfire and atmospheric physical processes.

Computational fluid dynamics (CFD) techniques have been applied to numerically model the dynamic physical processes of wildfires. Multiphase models that resolve processes at centimetre to tens-of-centimetres scales have been developed (Larini *et al*. 1998; Zhou and Pereira 2000; Morvan and Dupuy 2004; Zhou *et al*. 2005*a*, 2005*b*) as well as landscape-scale, 3-D models that resolve processes at metre to tens-of-metres scales (Linn 1997; Linn and Cunningham 2005; Mell *et al*. 2005, 2007; Cunningham and Linn 2007). Empirical fire spread algorithms from operational models have also been incorporated in a coupled wildfire–atmosphere mesoscale model (Clark *et al*. 2004).

HIGRAD/FIRETEC is a landscape-scale wildfire CFD model comprised of an atmospheric fluid dynamics model (HIGRAD) coupled to a wildfire physics model (FIRETEC). HIGRAD/FIRETEC is based on numerical representations of physical phenomena that occur in wildfires including mass and momentum transport, energy transport with radiative and convective heat transfer, turbulence and combustion. Despite the availability of modern parallel computing resources, constraints on grid-refinement due to computational costs force the simplification of combustion chemistry models in HIGRAD/FIRETEC and impose the challenge of developing and applying sub-grid modelling techniques to account for unresolved temporal and spatial variations in wildfire combustion.

The purpose of this paper is to describe the incorporation of a sub-grid model that is based on the mixture–fraction concept and that utilises a thermodynamic equilibrium model to account for gas phase combustion in HIGRAD/FIRETEC. First, brief descriptions are given of the previously implemented FIRETEC combustion chemistry models. Next, the mixture–fraction approach to modelling gas phase combustion is explained and a detailed description of the new sub-grid model development is given. Simulation results are then presented for wildfires in grass, California chaparral and ponderosa pine to demonstrate the performance of this new approach.

FIRETEC combustion models

FIRETEC does not explicitly model the kinetics of combustion reactions because temporal and spatial scales of these reactions

 10.1071/WF07116 1049-8001/10/020202

are not resolved. Sub-grid modelling is used to account for the physics of combustion chemistry in wildfires. Two FIRETEC chemistry models have been developed and reported in the literature. A brief description of these two models is included in this paper to provide some background for the description of the new sub-grid mixture–fraction-based chemistry model.

'Local' combustion model

The original combustion model developed for FIRETEC (Linn 1997) (referred to hereafter as the 'local' model) accounted for all combustion reactions with a single rate equation, which was meant to encompass the effects of pyrolysis, volatiles combustion and char oxidation.

$$F = c_F \frac{\overline{\hat{\rho}}_f \overline{\hat{\rho}}_o \sigma_{cm} \Psi_s}{\rho_{ref} s_x^2} \lambda_{of} \tag{1}$$

The reaction rate, F, is determined by the local bulk density of solid fuel ($\overline{\hat{\rho}}_f$), the bulk density of oxygen available in the gas phase ($\overline{\hat{\rho}}_o$), the turbulent diffusivity (σ_{cm}), and a probability density function (PDF, Ψ_s), which is a slightly modified form of the integrated Gaussian distribution. The caret above the density terms indicates that the quantity has been spatially averaged over the cell volume and the over bar indicates that the quantity is an ensemble average over many temporal realisations.

The PDF, Ψ_s used in Eqn 1 is an assumed distribution of temperature within a computational cell. Since grid resolution is at metre-length scales, it is possible for some portions of a cell to be hot and reacting while other portions of the cell are not. The acknowledgement and attempt to account for the temperature heterogeneity in the context of a mixing limited model is the essence of sub-grid combustion modelling in FIRETEC. Also note that Eqn 1 includes the bulk density of solid fuel. As a result, combustion reactions can only occur locally in the model where solid fuel is present. This precludes chemical reaction and therefore the production of heat, in computational cells above the fuel bed. The approximation that this model makes is that the heat is released within the same resolved volume as the solid fuel. In the context of large cells, this assumption is very reasonable but it is clearly an approximation in the context of intense fires and metre-scale cells since flame lengths can be tens-of-metres. It is not clear what impact this has on the representation of the nature of the fire, but one way to investigate the impact is to compare the results of this local model to a model that resolves the chemistry more explicitly.

'Nonlocal' combustion model

A two-equation model, which models pyrolysis and gas phase combustion separately, was also proposed for FIRETEC (Linn 1997), and a modified version of this proposed model was implemented in FIRETEC (Colman and Linn 2005). A transport equation for combustible, hydrocarbon-like gas species was added allowing for gas phase reactions to occur in any cell where combustible gas (hereafter referred to as hydrocarbons) may be present with oxygen. Since this type of reaction model is no longer localised to the fuel bed, it is referred to as the 'nonlocal' model. The two rate expressions for solid and gas reactions are quite similar in form to the original single-equation rate expression (Colman and Linn 2005).

$$F_{solid} = \frac{c_F \overline{\hat{\rho}}_f \sigma_{cm} \Psi_s}{s_x^2} \tag{2}$$

$$F_{gas} = \frac{\overline{\hat{\rho}}_{HC} \overline{\hat{\rho}}_o \sigma_{cm} \Psi_g}{2(N_o \hat{\rho}_{HC} + N_{HC} \overline{\hat{\rho}}_o)} \tag{3}$$

Mixture–fraction thermodynamic equilibrium model

This work centres on incorporating a mixture–fraction model based on thermodynamic equilibrium into FIRETEC as a third approach to modelling gas phase combustion chemistry. The motivation for this work is to apply this mixture–fraction approach to FIRETEC in order to take advantage of a thermodynamic equilibrium model to predict more complex combustion chemistry in the gas phase.

A mixture–fraction approach is one method of modelling turbulence chemistry interactions in combustion. The mixture–fraction is defined as the local fraction of mass that originates from a designated primary fuel source (Turns 2000). In the simplest application of the mixture–fraction approach, all other mass originates from a secondary source – ambient air in the case of wildfires. The physical and chemical properties of both the primary and secondary sources must be known at a chosen reference temperature and pressure. Given these known properties of the primary and secondary sources and a specified value of the mixture–fraction for any reacting mixture, the thermodynamic equilibrium solution for product temperature and species composition can be obtained.

Thermodynamic equilibrium solutions can be used in place of chemical rate equations in the combustion model assuming that the time scales of gas phase combustion reactions are sufficiently faster than the time scales of mixing (i.e. mixing-limited reactions) and that combustion reactions proceed completely to thermodynamic equilibrium. This method provides detailed predictions of chemical species production for a fraction of the computational cost that would be required to solve a complex kinetic mechanism.

Turbulence and chemistry are dynamically coupled in gas phase combustion. In highly resolved models (cm to mm length scales) where the mixture–fraction approach is traditionally applied, the interaction of turbulence with chemistry is modelled by using a probability density function (PDF) for the mixture–fraction. Functions that have been used for this PDF include the 'top hat, clipped Gaussian, β functions, multiple δ functions, as well as others' (Smoot and Smith 1985). The mean and variance of the mixture–fraction are transported quantities with the variance in the mixture–fraction explicitly coupled to the turbulent kinetic energy and the turbulent dissipation. It must be emphasised that the PDF mixture–fraction approach to modelling turbulence chemistry interactions is typically used in applications where flame sheets are resolved. For example, the PDF mixture–fraction thermodynamic equilibrium method has been used successfully in coal and gas combustor modelling applications to predict the combustion flame temperature and product chemical species without significant computational burden (Smoot and Smith 1985; Pitsch 2006). In these combustor

modelling applications, the computational grid is fine enough to resolve the length-scales of flame sheets and turbulence-induced fluctuations (intermittency) that impact gas phase combustion.

In landscape-scale wildfire modelling, it is not currently possible to resolve flame sheets and therefore it is not possible to explicitly model the coupling of turbulence and chemistry. For this reason, it is a significant challenge to apply a mixture–fraction thermodynamic equilibrium approach in modelling landscape-scale wildfire behaviour where neither the length-scales of flame sheets nor flame sheet intermittency are resolved. One approach to implementing the mixture–fraction model relies on the assumption of a constant stoichiometric value of the mixture–fraction at the flame sheet interface (Mell *et al*. 2007). The approach in this work allows the flame sheet mixture–fraction to vary. The motivation for implementing this type of approach is the desire for a more detailed gas phase combustion model without adding significant computational burden to the overall CFD model.

Sub-grid pocket model

Computational costs constrain grid refinement in HIGRAD/FIRETEC, limiting resolution to length scales on the order of 1 m. Since the physics and chemistry of combustion occur at length scales that are not resolved in HIGRAD/FIRETEC, it becomes necessary to utilise sub-grid models to account for these phenomena. To facilitate the application of the mixture–fraction model to HIGRAD/FIRETEC, a new sub-grid model was conceived and developed in order to account for the fact that volatiles and oxygen are not homogeneously distributed within the cells.

The products of solid pyrolysis are a mixture of gases including combustible hydrocarbon-like species. It is assumed that these combustible gases reside within spherical pockets, as illustrated in 2-D by the solid circle in Fig. 1, which is a simplified cartoon describing the mixing and reaction zone for gas phase chemical reactions. Part of the volume of the hydrocarbon pocket mixes with a volume of surrounding air and this mixture reacts to form product chemical species and produce a heat of reaction. It is assumed that the combustible gases from the hydrocarbon pocket and the volume of air mix rapidly to form a homogenous mixture at each numerical time step. The volume of this mixing layer around the spherical pockets depends on the radius of the pocket, r, and the length, $l + l \cdot a$, over which air and combustible gases mix, as depicted in Fig. 1 by the lightly shaded region. The pocket parameters also define the ratio of the volume of pure hydrocarbons from the pocket to the volume of air that comprise the reacting mixture. These parameters are meant to describe the notion of an area and thickness of a mixing zone at the interface of the volatiles-rich and oxygen-rich zones, in terms of the mass of volatiles in a computational cell. In this paper, the parameters r, l and a are not defined as functions of any specific resolved quantities in the hydrodynamics model; however, future research will investigate how these parameters depend on resolved quantities such as pyrolysis rate, inhomogeneity of fuels and turbulence. It is also anticipated that these parameters might evolve with time and space as volatiles transport (i.e. the pocket radius decreases as volatiles combust). With the pocket radius held constant in time and space, instead of tracking the changes that would occur in the pocket radius with shrinking pockets, it is assumed that the number of pockets decreases as gases react. By specifying r, l and a and solving for both the density of unreacted combustible gas (i.e. the number of pockets of combustible gas in a cell) and the mixture–fraction within a computational cell from transport equations, the local mixture–fraction of the reacting 'hydrocarbon-air mixture' can be calculated.

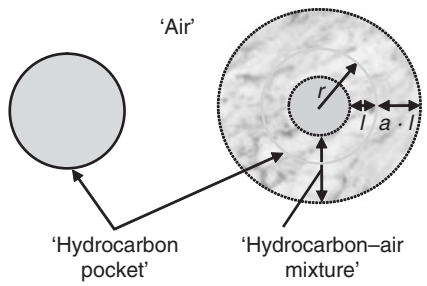

Fig. 1. Illustration of a sub-grid spherical 'pocket' of combustible gas mixing with surrounding air.

In the sub-grid pocket model illustrated in Fig. 1, the reacting mixture is composed of pure hydrocarbons (a portion of the pocket volume in the space from $r - l$ to r) and air (the volume surrounding the pocket in the space from r to $r + l \cdot a$). The reacting volumes of pure hydrocarbons, $V_{HC,r}$, and surrounding air, $V_{air,r}$, are calculated as follows (Clark 2008):

$$V_{HC,r} = \frac{4}{3}\pi r^3 - \frac{4}{3}\pi(r-l)^3 = \frac{4}{3}\pi(3lr^2 - 3l^2r + l^3) \quad (4)$$

$$V_{air,r} = \frac{4}{3}\pi(r+al)^3 - \frac{4}{3}\pi r^3 = \frac{4}{3}\pi(3alr^2 + 3a^2l^2r + a^3l^3) \quad (5)$$

The volume of reacting mixture is the sum of the volumes of reacting hydrocarbons and air:

$$V_{HC,r} + V_{air,r} = \frac{4}{3}\pi[(3l+3al)r^2 + (3a^2l^2 - 3l^2)r + a^3l^3 + l^3] \quad (6)$$

The fraction of reacting mixture that consists of pure hydrocarbons (χ) is calculated as:

$$\chi = \frac{V_{HC,r}}{V_{HC,r} + V_{air,r}} = \frac{3r^2 - 3lr + l^2}{(3+3a)r^2 + (3a^2l - 3l)r + a^3l^2 + l^2} \quad (7)$$

The volume fraction of reacting gases within a computational cell (ϕ_r) is given by:

$$\phi_r = \frac{N_{pockets}(V_{HC,r} + V_{air,r})}{V_{cell}} = \frac{\overline{\hat{\rho}}_{HC}\hat{V}_{HC}}{r^3} \times [(3l+3al)r^2 + (3a^2l^2 - 3l^2)r + a^3l^3 + l^3] \quad (8)$$

where the specific volume of reacting hydrocarbons is calculated assuming ideal gas, that is:

$$\hat{V}_{HC} = \frac{RT_{HC}}{M_{HC}P} \quad (9)$$

The densities of reacting hydrocarbons and air are respectively:

$$\rho_{HC,r} = \frac{\chi\phi_r}{\hat{V}_{HC}} = \frac{\chi\bar{\bar{\rho}}_{HC}[(3l+3al)r^2+(3a^2l^2-3l^2)r+a^3l^3+l^3]}{r^3} \quad (10)$$

and

$$\rho_{air,r} = \frac{(1-\chi),\phi_r}{\hat{V}_{air}} = \frac{(1-\chi)\bar{\bar{\rho}}_{HC}[(3l+3al)r^2+(3a^2l^2-3l^2)r+a^3l^3+l^3]}{r^3} \times \frac{\hat{V}_{HC}}{\hat{V}_{air}} \quad (11)$$

The ratio of the specific volume of hydrocarbons to air is assumed to be approximately one, since gases are assumed ideal and the temperatures and molecular weights of the hydrocarbons and air are similar:

$$\frac{\hat{V}_{HC}}{\hat{V}_{air}} = \frac{T_{HC}}{T_{air}}\frac{M_{air}}{M_{HC}} \approx 1 \quad (12)$$

This approximation simplifies the equation for the density of reacting air to quantities in the model that are either resolved or specified, yielding:

$$\rho_{air,r} = \frac{(1-\chi)\bar{\bar{\rho}}_{HC}[(3l+3al)r^2+(3a^2l^2-3l^2)r+a^3l^3+l^3]}{r^3} \quad (13)$$

The overall mixture–fraction in a computational cell is defined as the fraction of elemental mass in the cell that originated from a primary source:

$$\bar{f}_{cell} \equiv \frac{\bar{\bar{\rho}}_p}{\bar{\bar{\rho}}_p + \bar{\bar{\rho}}_s} \quad (14)$$

For wildfires, the primary source (indicated with the subscript p) is chosen as the production of hydrocarbons from pyrolysis. The chemical and physical properties of this primary material are calculated at 700 K for the gas mixture described in Colman and Linn (2005). It is assumed that the spherical pockets contain only pure, unreacted primary material; therefore, the mixture–fraction of these pockets, $f_{HCpocket} = 1$. The mixture–fraction of the air in the cell is:

$$f_{air} = \frac{\rho_{p,air}}{\overline{\rho} - \bar{\bar{\rho}}_{HC}} = \frac{\bar{f}_{cell}\overline{\rho} - \bar{\bar{\rho}}_{HC}}{\overline{\rho} - \bar{\bar{\rho}}_{HC}} \quad (15)$$

where the density of primary material in the air, $\rho_{p,air}$, is the mass of elements per cell volume that originated from pyrolysis, but reacted and no longer resides within spherical pockets. Finally, the mixture–fraction of the reacting mixture can be calculated:

$$f_r = \frac{f_{HCpocket}\rho_{HC,r} + f_{air}\rho_{air,r}}{\rho_{HC,r} + \rho_{air,r}} \quad (16)$$

The flame temperature and mole fractions of combustion products are obtained by interpolation from a look-up table of stored thermodynamic equilibrium calculations. The look-up table covers the entire range of possible mixture–fractions, $0 \le f_r \le 1$, and is generated before running the simulation. The heat of reaction is not calculated explicitly; rather, it is approximated using an energy balance. Assuming that all species have constant heat capacities equal to air and that conditions are adiabatic, the heat of reaction is equal to the change in sensible heat that results from the reaction. The flame temperature is used to estimate the change in sensible heat, calculated by multiplying the heat capacity of air by the difference between the flame temperature and the average gas temperature in the cell before reaction.

$$\Delta H_{rxn} \approx \Delta H_{sensible} \approx c_p(T_{flame} - \overline{T}_{gas}) \quad (17)$$

Eqn 17 might seem like an oversimplification in modelling the energy produced during the gas phase combustion processes. However, the formulation of the energy equation in HIGRAD is cast in terms of potential temperature. Potential temperature is used in atmospheric sciences and is defined as 'the temperature that an unsaturated parcel of dry air would have if brought adiabatically and reversibly from its initial state to a standard pressure, ... typically 100 kPa' (American Meteorological Society 2007). The enthalpy of the total gas mixture could be calculated if the concentrations of all gas phase chemical species were explicitly tracked. Lacking the necessary detail for a thermodynamically consistent method of converting from potential temperature to enthalpy, Eqn 17 is used to approximate the change in energy due to gas phase combustion.

Numerical simulations

A suite of HIGRAD/FIRETEC simulations was performed using the implemented mixture–fraction model for gas phase combustion. The HIGRAD/FIRETEC model employs a numerical integration scheme to solve the transient conservation equations for mass, momentum, energy and species (oxygen) in the gas phase, and conservation of mass for fuel, moisture and energy in the solid phase. A turbulence model is also implemented. The HIGRAD/FIRETEC modelling approach is described more extensively by Linn and Cunningham (2005) and Linn (1997).

Fire spread was simulated in three fuel beds: grass, California chaparral and ponderosa pine. Four simulations were performed for each fuel bed with inlet wind velocities of 1, 3, 6 and 12 m s^{-1} for a total of 12 simulations. The domain for all simulations was 320 × 320 × ~600 m. The horizontal dimensions of the grid were uniform with grid cells spaced 2 m apart. The vertical dimensions of the grid were stretched with increasing vertical height within the computational domain. The ground layer of grid cells had a vertical dimension of 1.5 m, while the top layer of grid cells had a vertical dimension of 40.8 m. All fuel beds covered the entire surface of the domain, the topography was flat and a neutral atmospheric stability was assumed. The pocket parameters for the sub-grid mixture–fraction model were held constant and specified at $r = 0.01$ m, $l = 0.67 \cdot r$ and $a = 2.5$. The net effect of these parameters is to specify the volume of the reacting zone for known amounts of hydrocarbons. These pocket parameter

values were chosen because they yielded reasonable and stable numerical predictions of propagating wildfire flame fronts. However, future work is needed to more formally determine the sensitivity of the results to these parameters.

Description of fuel beds

Grass fuel beds consisted of evenly distributed grass at a height of 0.7 m covering the entire ground layer surface of the domain. The fuel loading for grass was 0.7 kg m^{-2} and the initial moisture content of the grass was 5%. Moisture contents were given on a dry-fuel basis. The surface area per unit volume of fuel was 4000 m^{-1}. The grass fuel bed specifications in this work followed the specifications described by Linn and Cunningham (2005).

The fuel bed for ponderosa pine simulations was modelled similarly to a previously reported method (Linn *et al*. 2005). It consisted of a ponderosa pine canopy distributed across the fuel layer based on measurements that included detailed tree location data from a plot surveyed by the USDA Forest Service Rocky Mountain Research Station. The maximum canopy height was 19.9 m, the average canopy bulk density was ~0.12 kg m^{-3} and the initial moisture content of the canopy was specified as 130%. Ground layer fuels were distributed below the canopy: litter with a moisture content of 10% below the canopy and grass with a moisture content of 5% in areas where the canopy was thinner or open. The maximum bulk density of both grass and litter was 1.0 kg m^{-3}.

The fuel bed for chaparral simulations was modelled using the same routine used for ponderosa pine simulations. However, in the case of the chaparral fuel beds, the fuel distribution was not based on data from specific field surveys. The average crown diameter was 2.5 m with 60% coverage and shrub heights 1–2 m. The initial fuel moisture content for the canopy was specified as 130%. For the ground layer fuels, the specified moisture contents were 5% for grass and 10% for litter.

Ignition for all simulations began along a 100 m-long and 4 m-wide strip at a location 60 m downwind from the wind inlet boundary and centred in the crosswind direction of the domain. Within this strip of the computational domain, the solid temperature was artificially increased from 300 to 1000 K over 2 s of simulated time. This ignition method was consistent with previous simulations performed using the 'local' and 'nonlocal' models (Colman and Linn 2005; Linn and Cunningham 2005).

Combustible gas properties

The properties of the combustible gas were specified based on the composition of the hydrocarbon-like gas mixture used in the 'nonlocal' model (Colman and Linn 2005). This gas composition was based on analyses of rapid pyrolysis products for both cellulose and lignin by previous researchers (Hajaligol *et al*. 1982; Nunn *et al*. 1985). Based on these analyses, the elemental composition of the pyrolysis products was assumed to be: 37% (w/w) carbon, 7% (w/w) hydrogen and 56% (w/w) oxygen.

The species composition of the primary material stream used in the mixture–fraction model is in Table 1. The same primary stream properties were used for grass, chaparral and ponderosa pine simulations in this work, but one could specify primary stream properties based on the compositions of individual fuel types.

Table 1. Composition of hydrocarbon-like combustible gas used in mixture–fraction model simulations

Species	% (w/w)	Species	% (w/w)
CO_2	16.04	C_2H_4	3.49
H_2O	15.97	C_2H_6	0.50
CO	46.87	C_3H_6	1.05
H_2	2.49	CH_3OH	3.98
CH_4	5.98	CH_3CHO	3.65

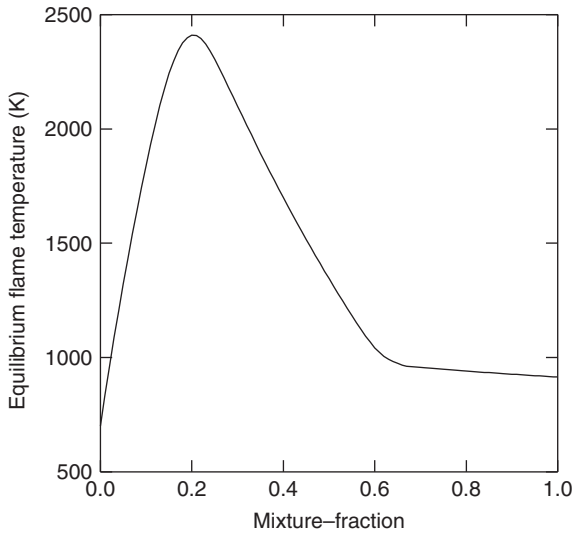

Fig. 2. Equilibrium flame temperature as a function of mixture–fraction for the combustion of 'hydrocarbons' with air.

Mixture–fraction thermodynamic equilibrium look-up table

The NASA Chemical Equilibrium with Applications program (McBride and Gordon 1996) was adapted and used to generate a look-up table of thermodynamic equilibrium solutions covering the range of mixture–fractions, $0 \leq f_r \leq 1$. The input primary material was specified by weight percent of species as listed in Table 1 at an initial temperature of 700 K. The input secondary material was specified as air (76.7% (w/w) N_2, 23.3% (w/w) O_2), also at a temperature of 700 K. This initial temperature of 700 K was chosen to roughly approximate the thermodynamic conditions of pre-heated reactants within the vicinity of gas phase wildland fire combustion. Such an approximation was necessary due to the form of the energy equation in HIGRAD, which was cast in terms of potential temperature rather than enthalpy.

Product species considered in the equilibrium solution routine in this study were limited to CH_4, CO_2, H_2, NH_3, N_2, OH, C (solid), CO, H, H_2O, NO, O and O_2; however, it is possible to consider any chemical species by either using the extensive NASA library of thermodynamic properties or manually specifying the

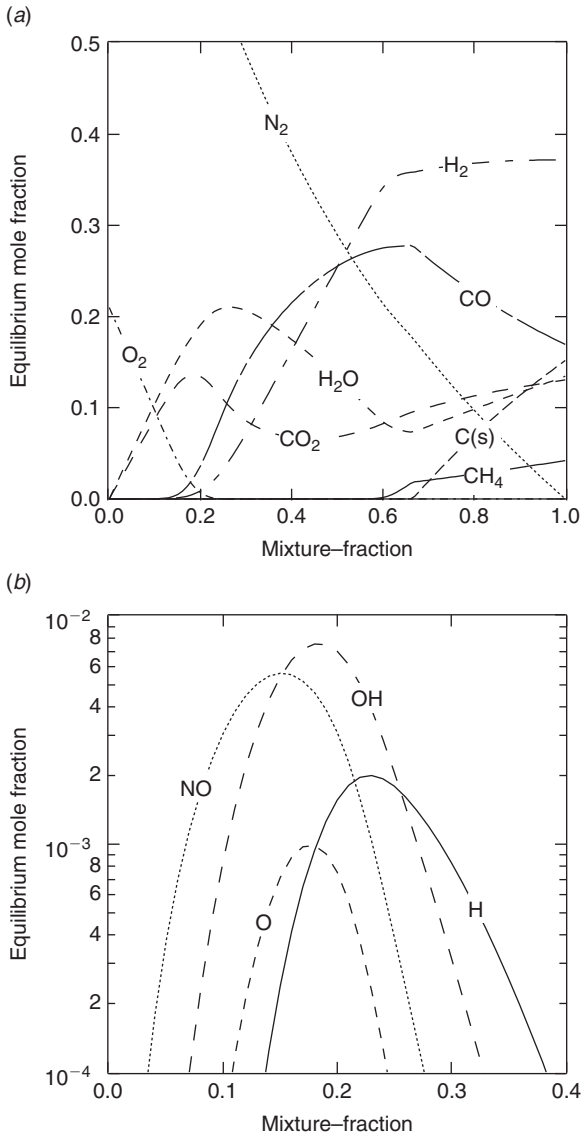

Fig. 3. Equilibrium product species mole fractions as a function of mixture–fraction for the combustion of the selected hydrocarbon mixture with air. Major (*a*) and minor species (*b*) with NH_3 excluded because its mole fraction was less than 10^{-4}.

thermodynamic properties of the species. From the generated look-up table of thermodynamic equilibrium solutions, values of combustion flame temperatures as a function of mixture–fraction are in Fig. 2. Note that the peak flame temperature occurs at or near the stoichiometric value of the mixture–fraction, which is 0.188 in this case. Also note that at a mixture–fraction of 1.0, pure fuel is predicted to react and result in a temperature higher than the initial temperature of 700 K. This is due to presence of oxygen within the fuel, which could theoretically react with the carbon and hydrogen in the fuel to produce heat.

Values of product species mole fractions are in Fig. 3 with major species plotted in Fig. 3*a* and minor species plotted in Fig. 3*b*. Near the stoichiometric mixture–fraction, the primary products of combustion are CO_2 and H_2O. However, at more

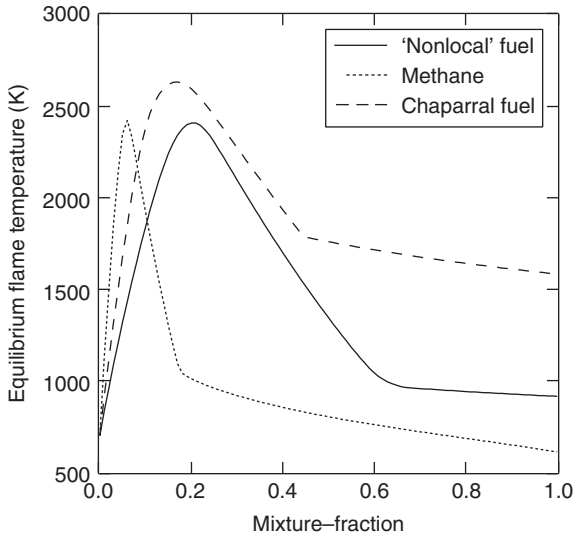

Fig. 4. Comparison of predicted adiabatic equilibrium flame temperatures for the combustible gas mixture used in the 'nonlocal' and sub-grid pocket models, methane and a combustible gas mixture from chaparral, assuming the same elemental composition as the unburned foliage.

fuel-rich mixture–fractions greater than 0.2, CO and H_2 become significant combustion products. At very fuel-rich mixture–fractions greater than 0.6, CH_4 and C (solid) are predicted equilibrium products. C (solid) could be thought of as a soot-precursor species and the prediction of C (solid) production using the mixture–fraction equilibrium model may provide an avenue to incorporation of a simple soot production and transport model.

Equilibrium flame temperature predictions for the selected hydrocarbon mixture were compared with predicted flame temperatures for methane and for a fuel of elemental composition based on standard ultimate analysis of the foliage of four California chaparral species (Pickett 2008), which had an average elemental composition of 52.17% carbon, 6.43% hydrogen, 1.29% nitrogen and 40.11% oxygen (w/w, dry ash free basis). Initial reactant temperatures were 700 K, and the species considered at chemical equilibrium were limited to CO, CO_2, H, H_2, H_2O, NO, N_2, O, OH, O_2, NH_3, CH_4, C (solid), HCN, HNC, NO_2 and C_2H_2. Note that four additional species were considered in this comparison (HCN, HNC, NO_2 and C_2H_2) as the presence of these species became significant in order to obtain converged equilibrium solutions for the methane and California chaparral fuel types. A comparison of flame temperatures for the three different primary streams is in Fig. 4.

Computational resources used

Numerical simulations were performed on large-scale Linux clusters at Los Alamos National Laboratory. Each numerical simulation was run on 64 AMD 2.6 GHz Opteron processors with ~6 h of compute time on 64 processors required to simulate 150 s of real time. The compute time for the sub-grid pocket model was 7% higher than the 'local' FIRETEC model and 3% higher than the 'nonlocal' FIRETEC model.

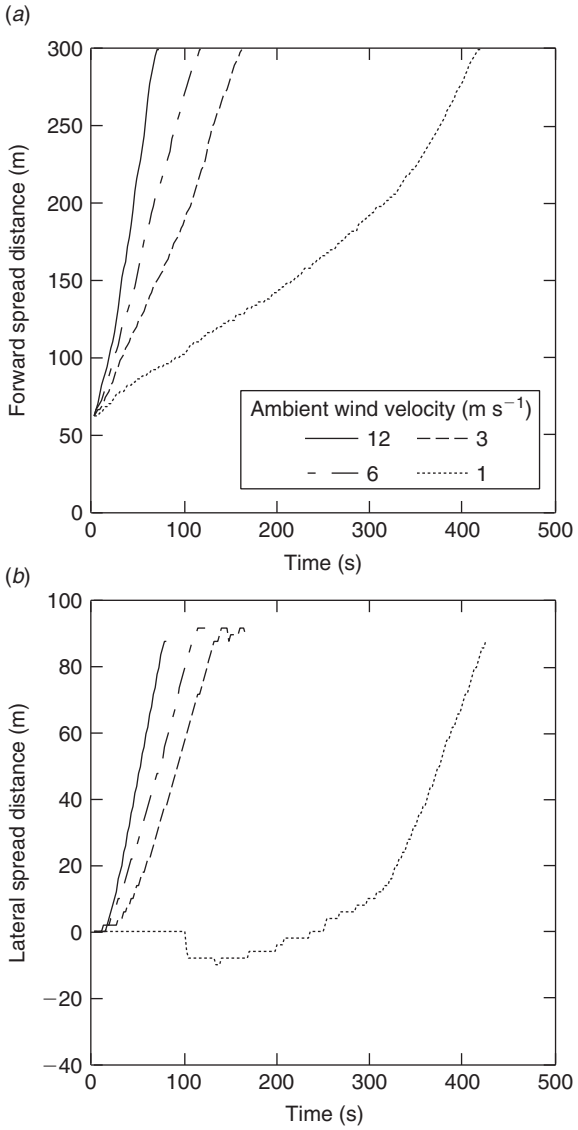

Fig. 5. Downwind spread distance *v.* time from simulated grass fires (*a*). Lateral spread distance *v.* time from simulated grass fires (*b*).

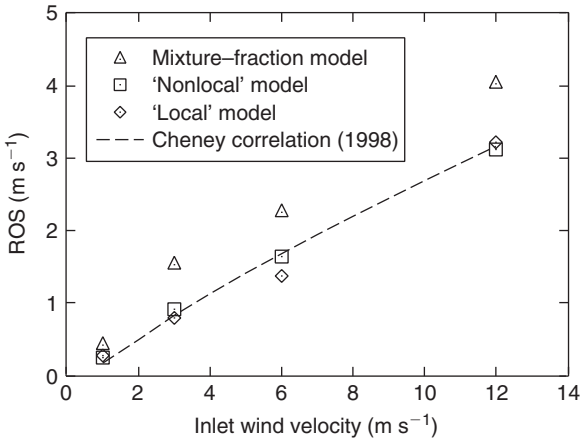

Fig. 6. Comparison of downwind spread rates in simulated grass fires. Results are shown from simulations of the three FIRETEC chemistry models: 'local', 'nonlocal' and the mixture–fraction models with a comparison to Cheney *et al.* (1998).

Grassfire results

Fire downwind spread distance was defined as the distance to the point farthest downwind where the solid temperature was above 500 K. Lateral spread distance was defined likewise for spread in the crosswind direction. Overall fire spread rates were determined by taking the time derivative of the downwind spread distance using simple linear regression. The downwind spread distance is plotted for four grass fire simulations (Fig. 5*a*). Lateral spread distance is in Fig. 5*b*. The simulations yielded a trend of more rapid fire spread at higher inlet wind velocities. In the 1-m s^{-1} simulation, the fire line narrowed initially indicated by the negative lateral spread distance. After this initial narrowing, the fire began to propagate with positive lateral spread and continued to spread laterally throughout the remainder of the simulation. This behaviour could be attributed to several factors in the coupled hydrodynamics–fire model; however, isolating the specific causes is beyond the scope of this paper.

Overall, fire spread rates from the mixture–fraction-based FIRETEC simulations are compared in Fig. 6 to previously reported spread rates from 'local' and 'nonlocal' FIRETEC simulations (Colman and Linn 2005) and to an empirical correlation for fire spread in undisturbed, 100% cured natural pasture grasslands (Cheney *et al.* 1998). A similar set of simulations was performed by Mell *et al.* (2007). In all cases, the mixture–fraction-based model produced simulated spread rates that were higher than the predicted spread rates from the 'local', 'nonlocal' and empirical models. Thus the results of the new mixture–fraction-based model are not necessarily better predictions of fire behaviour. One possible explanation for the higher rates of spread observed in the mixture–fraction model simulations is that the estimation for the heat of reaction was too high. This estimation can be improved in the future by making a better estimate or calculation of the initial reactant temperature; this work simply assumed the initial reactant temperature was 700 K. Also, the mixture–fraction-based pocket model parameters could be further refined following more formal sensitivity analysis in future work. These are two ways that could yield improvements to this new approach in the future.

A time history of oxygen and hydrocarbon mass fractions and potential temperature is in Fig. 7*a* and a time history of mixture–fraction, f_r, and equilibrium product species predictions of CO_2 and CO from the sub-grid pocket combustion model is in Fig. 7*b*. The model results shown in these plots were taken from the 12-m s^{-1} inlet wind grassfire simulation at a point located in the centre of the domain and within the fuel bed (i.e. computational cell number [80, 80, 1] out of a domain of 160 × 160 × 41 cells). Fig. 7*a* shows that as the fire front approaches the point, the potential temperature increases sharply, the oxygen mass fraction decreases to a minimum and the hydrocarbons mass fraction increases to a maximum. This occurs as combustible hydrocarbons are produced via pyrolysis and then subsequently react in the gas phase. Fig. 7*b* shows that as the fire front approaches the

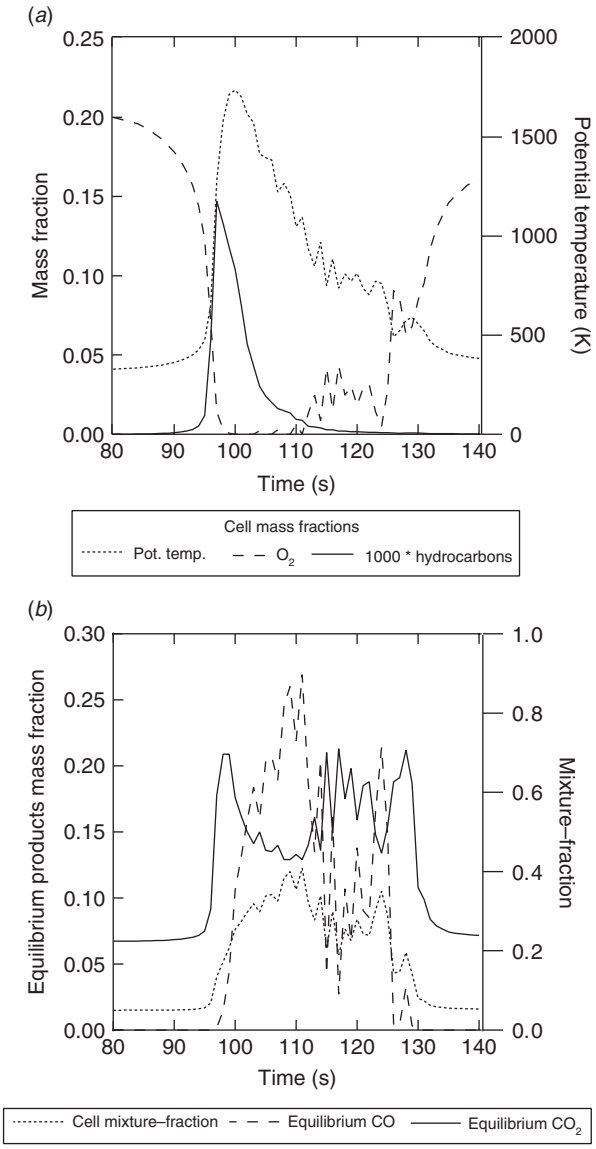

Fig. 7. Time histories for one point located in the fuel bed and in the centre of the domain for a grass fire simulation at 12 m s^{-1} inlet wind velocity. Cell mass fractions of gas phase oxygen and hydrocarbons are plotted on the left-hand ordinate (*a*) with potential temperature plotted on the right-hand ordinate. Note that the value of the hydrocarbons mass fraction is multiplied by 1000 for it to be visible on the same scale as the oxygen mass fraction. The predicted equilibrium mass fractions of combustion products CO_2 and CO are plotted on the left-hand ordinate (*b*) with mixture–fraction, f_r, plotted on the right-hand ordinate.

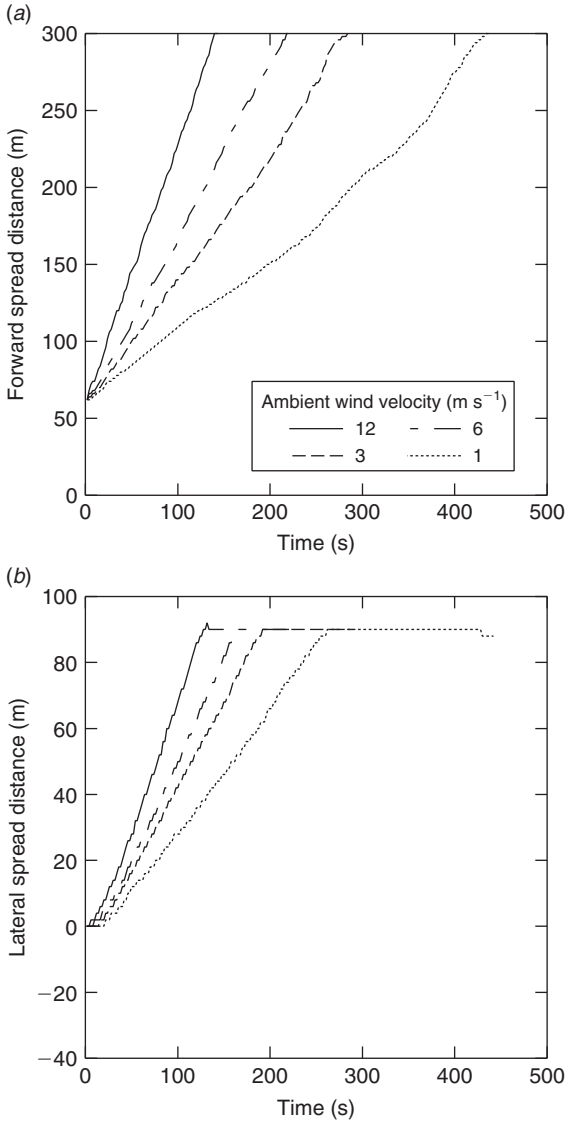

Fig. 8. Downwind spread distance *v.* time from simulated chaparral fires (*a*). Lateral spread distance *v.* time from simulated chaparral fires (*b*).

point, the sub-grid pocket combustion model begins to predict CO_2 and CO as equilibrium combustion products. Note that the peaks in the product mass fraction of CO correspond with the peaks in the mixture–fraction. As shown in Fig. 3*a*, CO production is generally enhanced under fuel-rich conditions (i.e. higher values of the mixture–fraction). For this reason, as the mixture–fraction reaches a maximum, the CO equilibrium product mass fraction also reaches a maximum. It should be noted that the mixture–fraction never reached a value greater than 0.6 and C (solid) was not predicted in the equilibrium products. Therefore, relying on the prediction of C (solid) production as a soot precursor would not be useful in this case.

Chaparral and ponderosa results

Figs 8 and 9 show plots of downwind spread distance and lateral spread distance for chaparral and ponderosa pine simulations preformed using the mixture–fraction model. Steady downwind and lateral spread was observed in all four chaparral simulations. However, in the ponderosa pine simulations, continuous downwind and lateral spread was only observed in the higher inlet wind velocity cases at 6 and 12 m s^{-1}. In the 3-m s^{-1} inlet wind velocity simulation, the fire propagated downwind but became narrower with time. The same behaviour was observed in the 1-m s^{-1} inlet wind velocity simulation, except in that case,

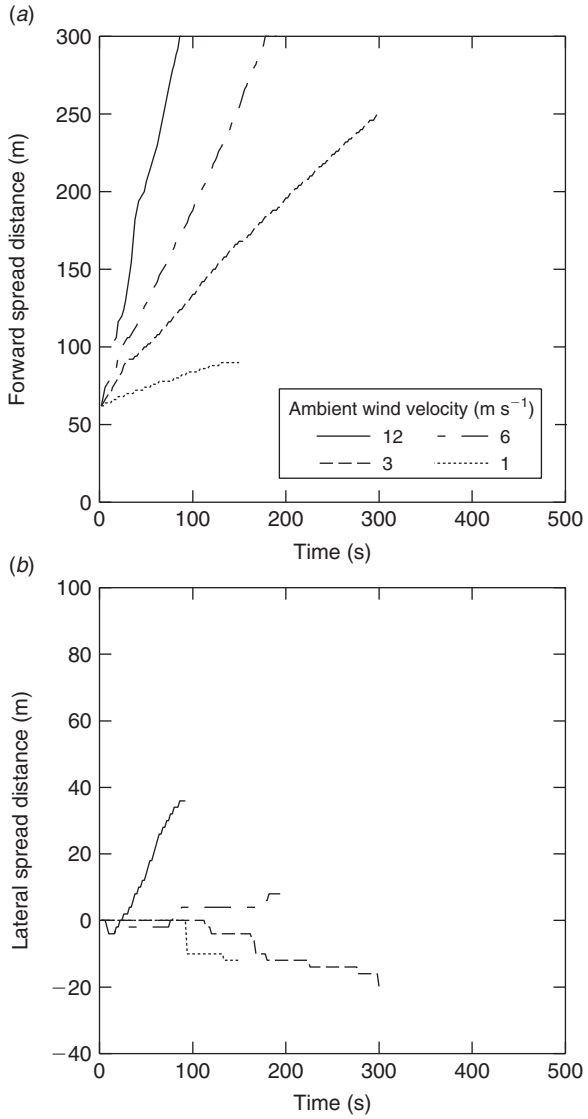

Fig. 9. Downwind spread distance *v.* time from simulated ponderosa pine fires (*a*). Lateral spread distance *v.* time from simulated ponderosa pine fires (*b*).

the narrowing caused the fire to quickly become extinguished. Little to no crowning occurred in the ponderosa pine simulations, perhaps due in part to the high moisture content (130%) specified for the canopy fuels.

Conclusions

A new sub-grid, gas phase chemistry model for FIRETEC was developed, implemented and demonstrated in a test suite of simulations that included grass, California chaparral and ponderosa pine fuel beds at inlet wind velocities of 1, 3, 6 and 12 m s^{-1}. This sub-grid model was based on the assumption that combustible gases reside within spherical pockets. Combustion flame temperatures and product species compositions were calculated assuming thermodynamic equilibrium. The modelled pocket parameters r, l and a were held constant in this study; however, future work will explore ways to allow these parameters, in particular the pocket radius (r) to vary dynamically with the combustion conditions. This would allow the fuel to air ratio to vary in the model but it is not clear what the implications would be for allowing these parameters to vary.

Grassfire simulation results were reasonable, compared with the simulation results of earlier FIRETEC models and the correlation from Cheney *et al*. (1998), thus demonstrating the feasibility of the model and potential for future development in this area of wildfire modelling research. The capability to predict many combustion products may allow for development of a soot transport model based on the fractions of soot precursor species produced by gas phase combustion. Currently, there is not an explicit soot production and transport model in FIRETEC, and perhaps having a method for predicting soot production would open up avenues for improving the radiative heat transfer model. Equilibrium predictions of CO and CO_2 from the simulation results were also shown. Though the mixture–fraction approach with equilibrium chemistry model predicts these and other combustion product species, conservation equations for individual species (other than oxygen) are not included in the overall hydrodynamics model. Nevertheless, the development of this mixture–fraction pocket model, which is capable of predicting detailed combustion product species, opens up future avenues for landscape-scale CFD wildfire model development.

Acknowledgements

This work was performed using the computing resources of the Los Alamos National Laboratory Institutional Computing Program at Los Alamos National Laboratory and the Fulton Supercomputing Laboratory at Brigham Young University. Financial support from the LANL Institute for Geophysics and Planetary Physics and the USDA Forest Service is also gratefully acknowledged.

References

American Meteorological Society (2007) 'Glossary of meteorology.' Available at http://amsglossary.allenpress.com/glossary/search?id=potential-temperature1 [Verified 28 November 2009]

Andrews PL, Bevins CD, Seli RC (2003) BehavePlus fire modeling system, version 2.0: user's guide. USDA Forest Service, Rocky Mountain Research Station, General Technical Report RMRS-GTR-106WWW. (Ogden, UT)

Cheney NP, Gould JS, Catchpole WR (1998) Prediction of fire spread in grasslands. *International Journal of Wildland Fire* **8**, 1–13. doi:10.1071/WF9980001

Clark MM (2008) A sub-grid, mixture–fraction-based thermodynamic equilibrium model for gas phase combustion in FIRETEC. PhD thesis, Brigham Young University, USA.

Clark TL, Coen J, Latham D (2004) Description of a coupled atmosphere–fire model. *International Journal of Wildland Fire* **13**, 49–63. doi:10.1071/WF03043

Colman JJ, Linn RR (2005) Separating combustion from pyrolysis in HIGRAD/FIRETEC. In 'Sixth Symposium on Fire and Forest Meteorology and the 19th Interior West Fire Council Meeting', 25–27 October 2005, Canmore, Alberta. Paper P1.22. (American Meteorological Society: Boston, MA)

Cunningham P, Linn RR (2007) Numerical simulations of grass fires using a coupled atmosphere–fire model: dynamics of fire spread. *Journal of Geophysical Research* **112**, D05108. doi:10.1029/2006JD007638

Finney MA (1998) FARSITE: fire area simulator–model development and evaluation. USDA Forest Service, Rocky Mountain Research Station, Research Paper RMRS-RP-4. (Ogden, UT)

Hajaligol MR, Howard JB, Longwell JP, Peters WA (1982) Product compositions and kinetics for rapid pyrolysis of cellulose. *Industrial & Engineering Chemistry Process Design and Development* **21**, 457–465. doi:10.1021/I200018A019

Larini M, Giroud F, Porterie B, Loraud JC (1998) A multiphase formulation for fire propagation in heterogeneous combustible media. *International Journal of Heat and Mass Transfer* **41**, 881–897. doi:10.1016/S0017-9310(97)00173-7

Linn RR (1997) A transport model for prediction of wildfire behavior. PhD thesis, New Mexico State University, USA.

Linn RR, Cunningham P (2005) Numerical simulations of grass fires using a coupled atmospheric–fire model: basic fire behavior and dependence on wind speed. *Journal of Geophysical Research* **110**, D13107. doi:10.1029/2004JD005597

Linn RR, Winterkamp J, Colman J, Edminster C, Bailey JD (2005) Modeling interactions between fire and atmosphere in discrete element fuel beds. *International Journal of Wildland Fire* **14**, 37–48. doi:10.1071/WF04043

McBride BJ, Gordon S (1996) Computer Program for Calculation of Complex Chemical Equilibrium Compositions and Applications: II. Users Manual and Program Description. National Aeronautics and Space Administration, NASA RP-1311. (Cleveland, OH)

Mell W, Charney JJ, Jenkins MA, Cheney P, Gould J (2005) Numerical simulations of grassland fire behavior from the LANL–FIRETEC and NIST–WFDS models. In 'EastFIRE Conference', 11–13 May 2005, Fairfax, VA. (George Mason University: Fairfax, VA)

Mell W, Jenkins MA, Gould J, Cheney P (2007) A physics-based approach to modelling grassland fires. *International Journal of Wildland Fire* **16**, 1–22. doi:10.1071/WF06002

Morvan D, Dupuy JL (2004) Modeling the propagation of a wildfire through a Mediterranean shrub using a multiphase formulation. *Combustion and Flame* **138**, 199–210. doi:10.1016/J.COMBUSTFLAME.2004.05.001

Nunn TR, Howard JB, Longwell JP, Peters WA (1985) Product compositions and kinetics in the rapid pyrolysis of milled wood lignin. *Industrial & Engineering Chemistry Process Design and Development* **24**, 844–852. doi:10.1021/I200030A054

Pickett BM (2008) Effects of moisture on combustion of live wildland forest fuels. PhD thesis, Brigham Young University, USA.

Pitsch H (2006) Large-eddy simulation of turbulent combustion. *Annual Review of Fluid Mechanics* **38**, 453–482. doi:10.1146/ANNUREV.FLUID.38.050304.092133

Rothermel RC (1972) A mathematical model for predicting fire spread in wildland fuels. USDA Forest Service, Intermountain Forest and Range Experiment Station, Research Paper INT-115. (Ogden, UT)

Smoot LD, Smith PJ (1985) 'Coal combustion and gasification.' (Plenum Press: New York)

Turns SR (2000) 'An Introduction to Combustion: Concepts and Applications.' (McGraw-Hill: New York)

Zhou XY, Pereira JCF (2000) Multidimensional model for simulating vegetation fire spread using a porous media sub-model. *Fire and Materials* **24**, 37–43. doi:10.1002/(SICI)1099-1018(200001/02)24:1<37::AID-FAM718>3.0.CO;2-Q

Zhou X, Mahalingam S, Weise D (2005*a*) Modeling of marginal burning state of fire spread in live chaparral shrub fuel bed. *Combustion and Flame* **143**, 183–198. doi:10.1016/J.COMBUSTFLAME.2005.05.013

Zhou X, Weise D, Mahalingam S (2005*b*) Experimental measurements and numerical modeling of marginal burning in live chaparral fuel beds. *Proceedings of the Combustion Institute* **30**, 2287–2294. doi:10.1016/J.PROCI.2004.08.022

Manuscript received 2 August 2007, accepted 9 September 2008

Appendix

Nomenclature used in this paper

a, flame-sheet thickness ratio
c_F, FIRETEC reaction rate coefficient
c_p, heat capacity ($J\,kg^{-1}\,K^{-1}$)
F, combined solid-gas reaction rate in FIRETEC ($kg\,m^{-3}\,s^{-1}$)
f_{air}, mixture-fraction of air in a computational cell (excludes unreacted, combustible, hydrocarbon-like gas)
$\bar{f}_{cell}$, mean mixture-fraction in a computational cell
F_{gas}, gas reaction rate in FIRETEC ($kg\,m^{-3}\,s^{-1}$)
$f_{HCpocket}$, mixture-fraction of spherical pockets composed of pure, unreacted, combustible, hydrocarbon-like gas; by definition equal to 1
f_r, mixture-fraction of reacting mixture
F_{solid}, solid reaction rate in FIRETEC ($kg\,m^{-3}\,s^{-1}$)
ΔH_{rxn}, heat of reaction ($J\,kg^{-1}$)
$\Delta H_{sensible}$, change in sensible heat ($J\,kg^{-1}$)
l, flame-sheet thickness parameter (m)
M_{air}, molecular weight of air ($kg\,mol^{-1}$)
M_{HC}, molecular weight of combustible, hydrocarbon-like gas ($kg\,mol^{-1}$)
N_{HC}, mass ratio of reactive gas that reacts with oxygen
N_o, mass ratio of oxygen that reacts with a reactive gas
P, pressure (atm)
r, radius of a spherical pocket of combustible, hydrocarbon-like gas (m)
R, gas constant ($m^3\,atm\,K^{-1}\,mol^{-1}$)
s_x, turbulent length scale (m)
T_{air}, temperature of reacting air (K)
T_{flame}, flame temperature predicted by chemical equilibrium (K)
$\overline{T}_{gas}$, average gas temperature (K)
T_{HC}, temperature of reacting, combustible, hydrocarbon-like gas (K)
$\hat{V}_{air}$, specific volume of reacting air ($m^3\,kg^{-1}$)
$V_{air,r}$, volume of reacting air (m^3)
$\hat{V}_{HC}$, specific volume of reacting, combustible, hydrocarbon-like gas ($m^3\,kg^{-1}$)
$V_{HC,r}$, volume of reacting combustible, hydrocarbon-like gas (m^3)

Greek symbols

λ_{of}, stoichiometric coefficient
π, mathematical constant
$\overline{\rho}$, total gas density ($kg\,m^{-3}$)
$\rho_{air,r}$, bulk density of reacting air ($kg\,m^{-3}$)
$\overline{\rho}_f$, bulk density of vegetation ($kg\,m^{-3}$)
$\overline{\rho}_{HC}$, mean bulk density of combustible hydrocarbon-like vapours in the gas phase ($kg\,m^{-3}$)
$\rho_{HC,r}$, bulk density of reacting, combustible, hydrocarbon-like gas ($kg\,m^{-3}$)
$\overline{\rho}_o$, mean bulk density of oxygen in the gas phase ($kg\,m^{-3}$)
$\overline{\rho}_p$, mean bulk density of primary mass in the gas phase ($kg\,m^{-3}$)
ρ_{ref}, reference density, $1\,kg\,m^{-3}$ ($kg\,m^{-3}$)
$\overline{\rho}_s$, mean bulk density of secondary mass in the gas phase ($kg\,m^{-3}$)
σ_{cm}, turbulent mixing term ($m^2\,s^{-1}$)
ϕ_r, volume fraction of reacting gas
χ, fraction of reacting mixture that consists of pure, combustible, hydrocarbon-like gas
Ψ_s, fraction of solid fuel that is above T_{crit}
Ψ_g, fraction of gaseous fuel that is above T_{crit}